IEEE Photonics Journal
An IEEE Photonics Society Publication

Open Access

Ultra-Sensitive Strain and Temperature Sensing Based on Modal Interference in Perfluorinated Polymer Optical Fibers

Volume 6, Number 5, October 2014

Goki Numata
Neisei Hayashi
Marie Tabaru
Yosuke Mizuno, Member, IEEE
Kentaro Nakamura, Member, IEEE

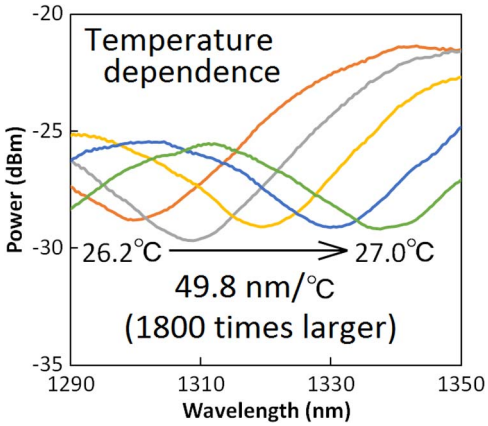

DOI: 10.1109/JPHOT.2014.2352637
1943-0655

Ultra-Sensitive Strain and Temperature Sensing Based on Modal Interference in Perfluorinated Polymer Optical Fibers

Goki Numata, Neisei Hayashi, Marie Tabaru, Yosuke Mizuno, *Member, IEEE*, and Kentaro Nakamura, *Member, IEEE*

Precision and Intelligence Laboratory, Tokyo Institute of Technology, Yokohama 226-8503, Japan

DOI: 10.1109/JPHOT.2014.2352637

Manuscript received July 16, 2014; accepted August 4, 2014. Date of publication August 28, 2014; date of current version September 11, 2014. This work was supported in part by Grants-in-Aid for Young Scientists (A) under Grant 25709032 and for Challenging Exploratory Research under Grant 26630180 from the Japan Society for the Promotion of Science (JSPS) and in part by research grants from the General Sekiyu Foundation, the Iwatani Naoji Foundation, and the SCAT Foundation. The work of N. Hayashi was supported by a Grant-in-Aid for JSPS Fellows under Grant 25007652. Corresponding author: Y. Mizuno (e-mail: ymizuno@sonic.pi.titech.ac.jp).

Abstract: We implement the strain and temperature sensors based on multimode interference in perfluorinated (PF) graded-index (GI) plastic optical fibers, and investigate their sensing performance at 1300 nm. We obtain strain and temperature sensitivities of -112 pm/$\mu\varepsilon$/m and $+49.8$ nm/°C/m, the absolute value of which are 12.9 and over 1800 times as large as those in silica GI multimode fibers, respectively. These ultra-high strain and temperature sensitivities probably originate from the unique core material, i.e., PF polymer.

Index Terms: Polymer optical fibers, perfluorinated polymer, modal interference, strain sensing, temperature sensing.

1. Introduction

Fiber-optic strain and temperature sensing has been an active research area because of light weight, small size, and insensitivity to ambient electromagnetic fields. While a number of methods exploiting fiber Bragg gratings (FBGs) [1], [2], long-period gratings (LPGs) [3], [4], Raman scattering [5], [6], and Brillouin scattering [7]–[11] have been developed, one of the simple and low-cost implementations is based on the interference among guided modes of a multimode fiber (MMF). Since Mehta *et al.* [12] reported the first demonstration in 2003, to date, various structures have been proposed, as well summarized in Table 1 in [13]. Among them, the most typical is a so-called single-mode-multimode-single-mode (SMS) structure [14]–[16], where an MMF is sandwiched between two single-mode fibers (SMFs).

Based on the SMS structure comprising a 1.8-m-long silica graded-index (GI-) MMF, Liu *et al.* [14] have obtained a strain sensitivity of $+10.3$ pm/$\mu\varepsilon$/m and a temperature sensitivity of $+32.5$ pm/°C/m at 1550 nm (corresponding to $+8.7$ pm/$\mu\varepsilon$/m and $+27.3$ pm/°C/m at 1300 nm, respectively). Tripathi *et al.* [15] have shown that not only the absolute values but also the signs of the strain and temperature sensitivities are highly dependent on the structure (e.g., core diameter) and the material (e.g., dopant) of silica MMFs. Recently, in order to enhance the maximal measurable strain, Huang *et al.* [17] have developed a large-strain sensor using a

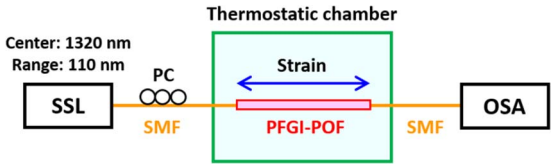

Fig. 1. Schematic of experimental setup. OSA, optical spectrum analyser; PC, polarization controller; PFGI-POF, perfluorinated graded-index plastic optical fiber; SMF, single-mode fiber; SSL, swept-source laser.

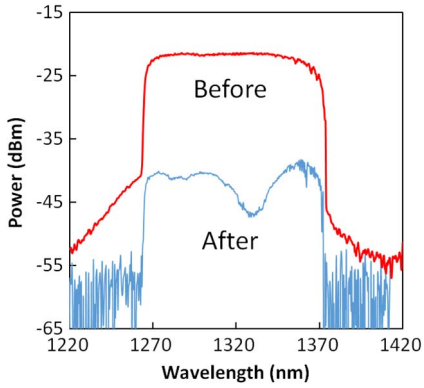

Fig. 2. Measured optical spectra before and after transmission through the POF.

0.16-m-long polymethyl methacrylate (PMMA)-based step-index plastic optical fiber (POF) as an MMF, and obtained strain and temperature sensitivities of -17.6 pm/$\mu\varepsilon$/m and $+581.9$ pm/$^\circ$C/m, respectively, at 1570 nm (corresponding to -14.6 pm/$\mu\varepsilon$/m and $+481.8$ pm/$^\circ$C/m at 1300 nm). However, the propagation loss of PMMA-based POFs at telecommunication wavelength is so high ($\gg 1 \times 10^5$ dB/km) that the maximal sensing range is inherently limited to several tens of meters. Besides, discriminative measurement of strain and temperature is also important for practical use; it can be theoretically achieved by combined use of multimode interference and another physical phenomenon, such as Brillouin scattering, which has, however, not been observed in PMMA-based POFs. Perfluorinated graded-index (PFGI-) POFs [18] are the only POFs that have a relatively low loss of $\sim$250 dB/km at 1550 nm (or $\sim$50 dB/km at 1300 nm) in which Brillouin scattering has been experimentally observed [19]–[22].

In this work, we implement the strain and temperature sensors based on the SMS structure comprising a PFGI-POF and investigate their sensing performance at 1300 nm. Three 1-m-long PFGI-POFs with core diameters of 50, 62.5, and 120 μm are used. When the core diameter is 62.5 μm, the strain sensitivity is -112 pm/$\mu\varepsilon$/m, the absolute value of which is 12.9 times as large as that in a silica GI-MMF. The temperature sensitivity at room temperature is $+49.8$ nm/$^\circ$C/m, which is over 1800 times as large as that in a silica GI-MMF.

2. Principle

The SMS structure consists of an MMF connected at both ends to identical SMFs. At the first SMF/MMF boundary, light is injected into the MMF through the lead-in SMF. As the spot size of the fundamental mode of the MMF is generally different from that of the SMF, the first few modes of the MMF are excited and propagate through the MMF with their respective propagation constants. At the second SMF/MMF boundary, the net field coupled from these modes to the lead-out SMF is determined by the relative phase differences among various modes of the MMF. When the fibers are axially aligned at the first SMF/MMF boundary, only the axially

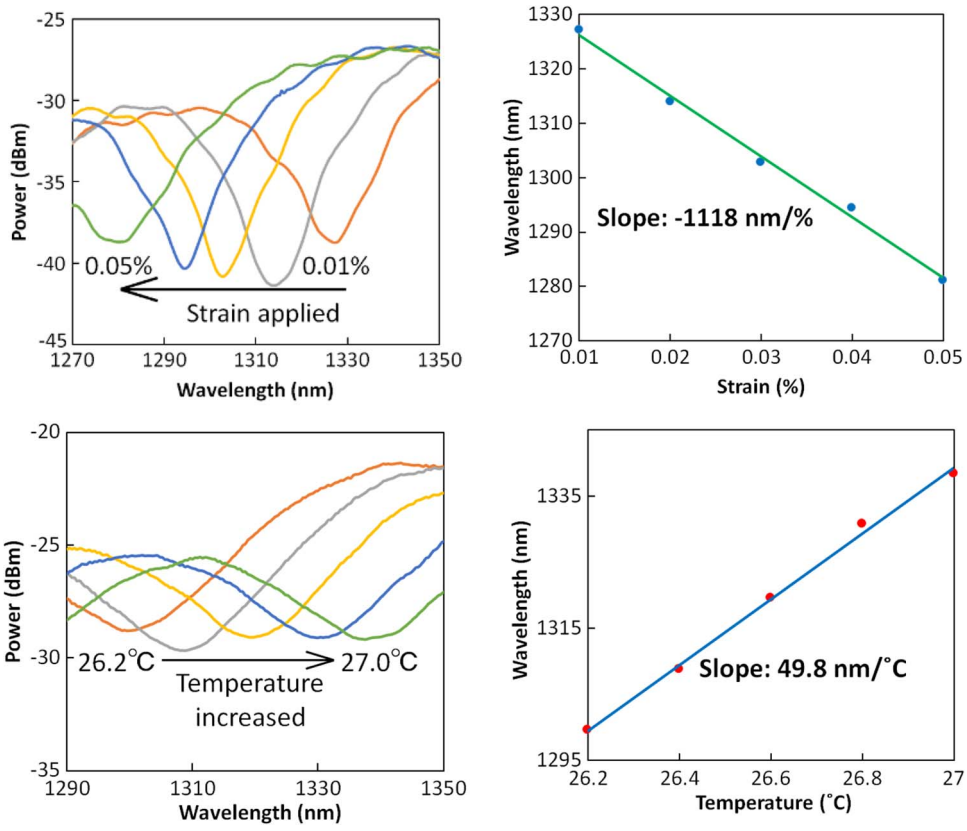

Fig. 3. Measurement results for the POF with 62.5-μm core. (a) Spectral dependence on strain, (b) dip wavelength versus strain, (c) spectral dependence on temperature, and (d) dip wavelength versus temperature.

symmetric modes of the MMF are excited. According to the detailed calculation [16], the optical power in the lead-out SMF can be expressed as

$$P_{\text{out}} = \left|a_1^2 + a_2^2 \exp i(\beta_1 - \beta_2)L + a_3^2 \exp i(\beta_1 - \beta_3)L + \ldots\right|^2 \quad (1)$$

where a_i is the field amplitude of the i-th mode at the first SMF/MMF boundary, β_i is the propagation constant of the i-th mode, and L is the length of the MMF. Equation (1) indicates that the optical power in the lead-out SMF is affected by physical changes (such as strain and temperature) influencing the propagation constants and/or the length of the MMF. By measuring this shift either in terms of power or the spectral location of peak/dip, the changes can be quantitatively obtained.

3. Experimental Setup

Three 1-m-long PFGI-POFs with different core diameters (50, 62.5, and 120 μm) were employed. The core and cladding layers are composed of doped and undoped polyperfluorobutenylvinyl ether, respectively. The refractive index at the center of the core is 1.356, whereas that of the cladding layer is 1.342 [23]; these values do not depend strongly on the optical wavelength [24]. The polycarbonate reinforcement overcladding layer (diameter: 500 μm) reduces microbending losses and increases the load-bearing capability. The numerical aperture is 0.185, and the propagation loss is $\sim$250 dB/km at 1550 nm and $\sim$50 dB/km at 1300 nm.

Fig. 1 depicts the experimental setup. The PFGI-POF was connected to silica SMFs by butt-coupling [19], i.e., the ends of the SMFs fitted with FC connectors were connected to both ends of the POF fitted with SC connectors via FC/SC adaptors. A swept-source laser (SSL) was used

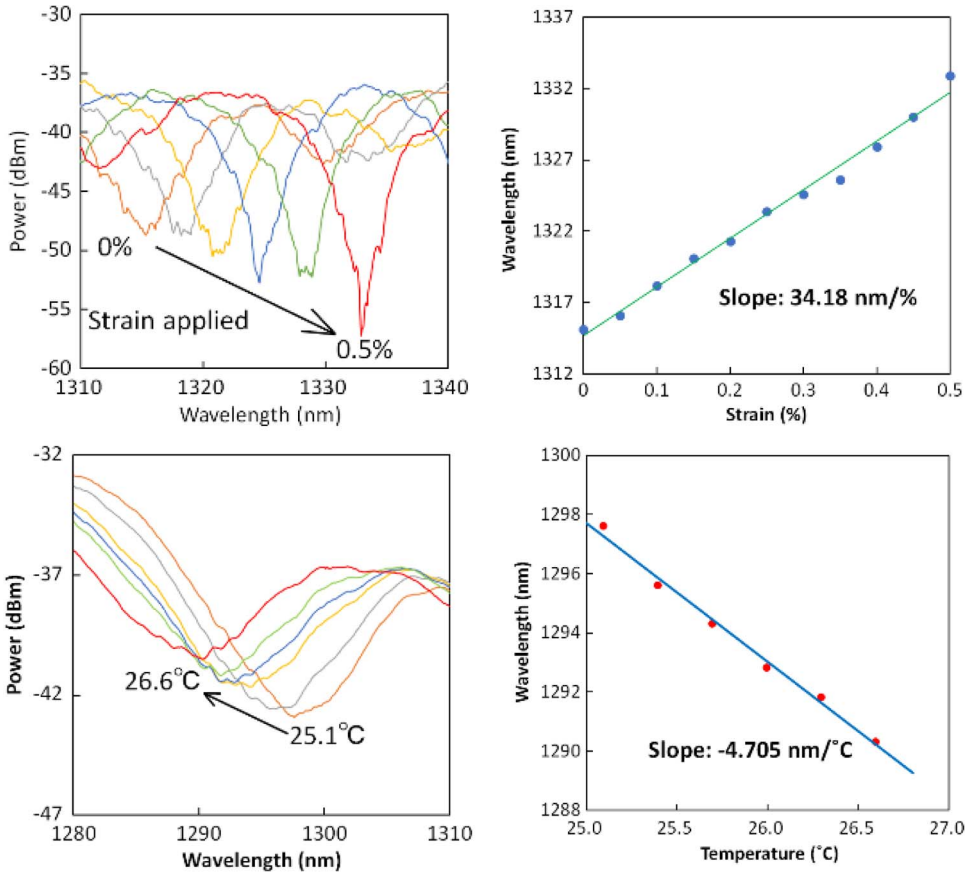

Fig. 4. Measurement results for the POF with 50-μm core. (a) Spectral dependence on strain, (b) dip wavelength versus strain, (c) spectral dependence on temperature, and (d) dip wavelength versus temperature.

as a light source, which can be regarded as a broadband source with a central wavelength of 1320 nm and a bandwidth of 110 nm. The laser output was, after polarization adjustment, launched into the PFGI-POF, and the transmitted light spectrum was monitored with an optical spectrum analyzer (OSA). Strain and temperature changes were applied to the whole length of the PFGI-POF. The room temperature was approximately 27 °C.

4. Experimental Results and Discussions

Fig. 2 shows the measured optical spectra before and after transmission through the PFGI-POF with 62.5-μm core diameter. A characteristic dip was clearly observed at around 1330 nm in the latter spectrum.

The measured dependence of this spectral dip on strain is shown in Fig. 3(a). With increasing applied strain, the spectral dip shifted to shorter wavelength. Fig. 3(b) shows the dip wavelength plotted as a function of strain. The dependence was almost linear with a coefficient of -1118 nm/%/m $(= -112$ pm/$\mu\varepsilon$/m$)$, the absolute value of which is approximately 12.9 and 7.7 times as large as those in a silica GI-MMF [14] and a PMMA-based POF [17], respectively. In the same way, as temperature increased, this spectral dip shifted to longer wavelength, as shown in Fig. 3(c). Fig. 3(d) shows the dip wavelength dependence on temperature, leading to a coefficient of $+49.8$ nm/°C/m, which is over 1800 and 100 times as large as those in a silica GI-MMF [14] and a PMMA-based POF [17], respectively.

We also performed the same measurement using the PFGI-POFs with 50-μm and 120-μm core diameters, as shown in Figs. 4(a)–(d) and 5(a)–(d), and obtained the strain and temperature

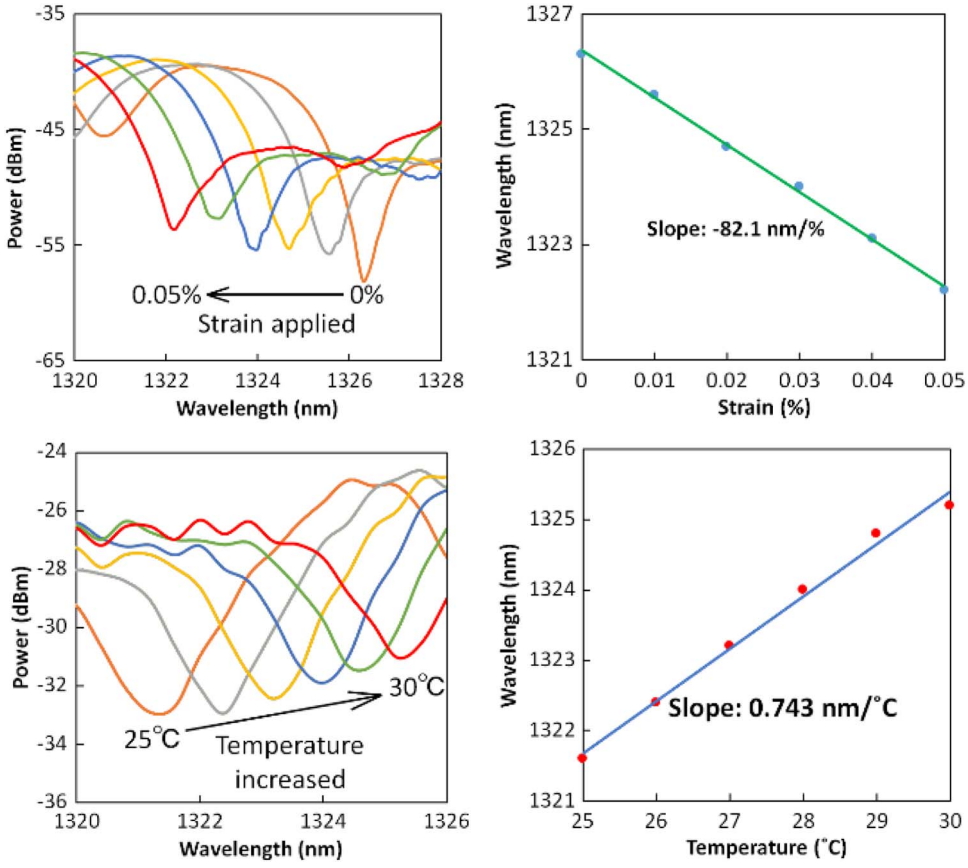

Fig. 5. Measurement results for the POF with 120-μm core. (a) Spectral dependence on strain, (b) dip wavelength versus strain, (c) spectral dependence on temperature, and (d) dip wavelength versus temperature.

coefficients of $+3.42$ pm/$\mu\varepsilon$/m and -4.71 nm/$^\circ$C/m (50-μm core), and -8.21 pm/$\mu\varepsilon$/m and $+0.74$ nm/$^\circ$C/m (120-μm core), respectively. These values were much larger than those in silica GI-MMFs with the same core diameters, but not as large as that in the PFGI-POF with 62.5-μm core diameter.

Considering that SMS-based sensors using silica GI-MMFs with the same core diameters do not have large strain and temperature coefficients, these ultra-high strain and temperature sensitivities of the PFGI-POF (especially with 62.5-μm core) probably originate not from its structure but from its unique material. In other words, the propagation constant of each mode and the length in perfluorinated polymer are much more highly dependent on strain and temperature than those in other MMFs (either glass or polymer).

5. Conclusion

The strain and temperature sensors based on modal interference in the SMS structure comprising a PFGI-POF was implemented, and their sensing performance was investigated using an SSL at around 1300 nm. When the core diameter was 62.5 μm, the strain and temperature sensitivities were -112 pm/$\mu\varepsilon$/m and $+49.8$ nm/$^\circ$C/m, the absolute values of which were 12.9 and $>$ 1800 times as large as those in a silica GI-MMF. We believe that the ultra-high temperature sensitivity of this sensor is quite attractive for such fields as will require precise temperature measurement. We also point out that the difference in sign between the strain and temperature coefficients will potentially lead to extremely accurate Brillouin-combined discriminative measurement of strain and temperature [25].

References

[1] A. D. Kersey *et al.*, "Fiber grating sensors," *J. Lightw. Technol.*, vol. 15, no. 8, pp. 1442–1463, Aug. 1997.
[2] B. O. Guan, H. Y. Tam, X. M. Tao, and X. Y. Dong, "Simultaneous strain and temperature measurement using a superstructure fiber Bragg grating," *IEEE Photon. Technol. Lett.*, vol. 12, no. 6, pp. 675–677, Jun. 2000.
[3] V. Bhatia and A. M. Vengsarkar, "Optical fiber long-period grating sensors," *Opt. Lett.*, vol. 21, no. 9, pp. 692–694, May 1996.
[4] Y. P. Wang, L. Xiao, D. N. Wang, and W. Jin, "Highly sensitive long-period fiber-grating strain sensor with low temperature sensitivity," *Opt. Lett.*, vol. 23, no. 23, pp. 3414–3416, Dec. 2006.
[5] M. A. Farahani and T. Gogolla, "Spontaneous Raman scattering in optical fibers with modulated probe light for distributed temperature Raman remote sensing," *J. Lightw. Technol.*, vol. 17, no. 8, pp. 1379–1391, Aug. 1999.
[6] M. N. Alahbani, Y. T. Cho, and T. P. Newson, "Simultaneous temperature and strain measurement with combined spontaneous Raman and Brillouin scattering," *Opt. Lett.*, vol. 30, no. 11, pp. 1276–1278, Jun. 2005.
[7] T. Horiguchi and M. Tateda, "BOTDA-nondestructive measurement of single-mode optical fiber attenuation characteristics using Brillouin interaction: Theory," *J. Lightw. Technol.*, vol. 7, no. 8, pp. 1170–1176, Aug. 1989.
[8] T. Kurashima, T. Horiguchi, H. Izumita, S. Furukawa, and Y. Koyamada, "Brillouin optical fiber time domain reflectometry," *IEICE Trans. Commun.*, vol. E76-B, no. 4, pp. 382–390, Apr. 1993.
[9] D. Garus, K. Krebber, F. Schliep, and T. Gogolla, "Distributed sensing technique based on Brillouin optical-fiber frequency-domain analysis," *Opt. Lett.*, vol. 21, no. 17, pp. 1402–1404, Sep. 1996.
[10] K. Hotate and T. Hasegawa, "Measurement of Brillouin gain spectrum distribution along an optical fiber using a correlation-based technique-proposal, experiment and simulation," *IEICE Trans. Electron.*, vol. E83-C, no. 3, pp. 405–412, Mar. 2000.
[11] Y. Mizuno, W. Zou, Z. He, and K. Hotate, "Proposal of Brillouin optical correlation-domain reflectometry (BOCDR)," *Opt. Exp.*, vol. 16, no. 16, pp. 12 148–12 153, Aug. 2008.
[12] A. Mehta, W. Mohammed, and E. G. Johnson, "Multimode interference-based fiber-optic displacement sensor," *IEEE Photon. Technol. Lett.*, vol. 15, no. 8, pp. 1129–1131, Aug. 2003.
[13] O. Frazao *et al.*, "Optical fiber refractometry based on multimode interference," *Appl. Opt.*, vol. 50, no. 25, pp. E184–E188, Sep. 2011.
[14] Y. Liu and L. Wei, "Low-cost high-sensitivity strain and temperature sensing using graded-index multimode fibers," *Appl. Opt.*, 46, no. 13, pp. 2516–2519, May 2007.
[15] S. M. Tripathi *et al.*, "Strain and temperature sensing characteristics of single-mode-multimode-single-mode structures," *J. Lightw. Technol.*, vol. 27, no. 13, pp. 2348–2356, Jul. 2009.
[16] A. Kumar, R. K. Varshney, C. S. Antony, and P. Sharma, "Transmission characteristics of SMS fiber optic sensor structures," *Opt. Commun.*, 219, no. 1–6, pp. 215–219, Apr. 2003.
[17] J. Huang *et al.*, "Polymer optical fiber for large strain measurement based on multimode interference," *Opt. Lett.*, vol. 37, no. 20, pp. 4308–4310, Oct. 2012.
[18] Y. Koike and M. Asai, "The future of plastic optical fiber," *NPG Asia Mater.*, vol. 1, no. 1, pp. 22–28, Oct. 2009.
[19] Y. Mizuno and K. Nakamura, "Experimental study of Brillouin scattering in perfluorinated polymer optical fiber at telecommunication wavelength," *Appl. Phys. Lett.*, vol. 97, no. 2, pp. 021103-1–021103-3, Jul. 2010.
[20] Y. Mizuno and K. Nakamura, "Potential of Brillouin scattering in polymer optical fiber for strain-insensitive high-accuracy temperature sensing," *Opt. Lett.*, vol. 35, no. 23, pp. 3985–3987, Dec. 2010.
[21] Y. Mizuno, N. Hayashi, and K. Nakamura, "Brillouin scattering signal in polymer optical fiber enhanced by exploiting pulsed pump with multimode-fiber-assisted coupling technique," *Opt. Lett.*, vol. 38, no. 9, pp. 1467–1469, May 2013.
[22] Y. Mizuno, N. Hayashi, H. Tanaka, K. Nakamura, and S. Todoroki, "Observation of polymer optical fiber fuse," *Appl. Phys. Lett.*, vol. 104, no. 4, pp. 043302-1–043302-4, Jan. 2014.
[23] M. Naritomi, H. Murofushi, and N. Nakashima, "Dopants for a perfluorinated graded index polymer optical fiber," *Bull. Chem. Soc. Jpn.*, vol. 77, no. 11, pp. 2121–2127, 2004.
[24] T. Ishigure, Y. Koike, and J. W. Fleming, "Optimum index profile of the perfluorinated polymer-based GI polymer optical fiber and its dispersion properties," *J. Lightw. Technol.*, vol. 18, no. 2, pp. 178–184, Feb. 2000.
[25] W. Zou, Z. He, and K. Hotate, "Complete discrimination of strain and temperature using Brillouin frequency shift and birefringence in a polarization-maintaining fiber," *Opt. Exp.*, vol. 17, no. 3, pp. 1248–1255, Feb. 2009.